A Quantitative Approach to Identify Morphological Features Relevant for Visual Function in Ranibizumab Therapy of Neovascular AMD

Philipp Roberts, Tamara Jasmin Mittermueller, Alessio Montuoro, Florian Sulzbacher, Marion Munk, Stefan Sacu, and Ursula Schmidt-Erfurth

Department of Ophthalmology and Optometry of the Medical University Vienna, Vienna, Austria

Correspondence: Ursula Schmidt-Erfurth, Department of Ophthalmology and Optometry of the Medical University Vienna, Waehringer Guertel 18-20, 1090 Vienna, Austria; ursula.schmidt-erfurth@meduniwien.ac.at.

See the appendix for the members of the Macula Study Group Vienna.

Submitted: March 3, 2014
Accepted: August 24, 2014

Citation: Roberts P, Mittermueller TJ, Montuoro A, et al. A quantitative approach to identify morphological features relevant for visual function in ranibizumab therapy of neovascular AMD. *Invest Ophthalmol Vis Sci*. 2014;55:6623–6630. DOI:10.1167/iovs.14-14293

Purpose. To quantitatively analyze morphological features in eyes with neovascular AMD (nAMD) at baseline, after 12 months, and after 24 months of intravitreal ranibizumab treatment and to perform a structure/function correlation.

Methods. Eyes with treatment-naïve nAMD were treated with intravitreal ranibizumab according to a standardized dosing regimen over 2 years and followed continuously in a prospective study design. The central foveal area of 1000 μm (horizontal) × 960 μm (vertical) of spectral-domain optical coherence tomography (SD-OCT) volume scans was evaluated quantitatively (using proprietary software) for the following pathologies: alteration of the external limiting membrane (ELM), alteration of the ellipsoid zone, subretinal fluid, pigment epithelium detachment, drusen, intraretinal cysts, subretinal mass, and subretinal pigment epithelium mass. The total area of each pathology was calculated in mm^2 at baseline and after 1 and 2 years of ranibizumab therapy and correlated with BCVA results.

Results. In total, 480 central SD-OCT scans of 20 consecutive patients were evaluated. In the multivariate regression analysis, the area of ELM alteration, the area of intraretinal cysts, and foveal retinal thickness were significant variables influencing visual acuity at baseline ($R = -0.827$; $R^2 = 0.684$; $P < 0.001$). The area of ELM alteration was the only significant factor to be directly associated with visual acuity at 12 months ($R = -0.846$; $R^2 = 0.716$; $P < 0.001$) and 24 months ($R = -0.778$; $R^2 = 0.606$; $P < 0.001$).

Conclusions. The integrity of the ELM appears to be the most important feature correlating with visual acuity in native nAMD as well as nAMD treated with intravitreal ranibizumab at each time interval, but not prospectively. In general, no significant predictors for an individual gain or loss in mid- (12 months) or long-term BCVA results (24 months) were found by OCT.

Keywords: ranibizumab, neovascular AMD, spectral-domain OCT

Age-related macular degeneration (AMD) is the most common cause of severe and irreversible vision loss in the elderly population in industrialized countries.[1–5] The neovascular form of AMD (nAMD) is characterized by the development of marked degrees of retinal edema, sub- or intraretinal fluid, hemorrhage, and/ or fibrous scarring, if left untreated.[6] Since the introduction of anti-VEGF agents, the visual prognosis of patients with nAMD has improved drastically.[7–10] The pivotal phase III studies testing the efficacy of intravitreal ranibizumab as treatment for nAMD have shown that monthly injections over the course of 2 years can halt disease progression in most patients.[10–12] Nevertheless, morphologic changes are also noted under therapy, and visual function demonstrates a huge variability between patients. In addition, simply due to the large number of patients, monthly injections appear to be difficult to implement in clinical practice for both logistical as well as economical reasons. Even though intravitreal injections are a safe procedure, every injection bears the risk of endophthalmitis; moreover, monthly administration of anti-VEGF agents is cost-intensive and was found to be associated with progressive geographic atrophy.[13,14] Flexible regimens rely on specified retreatment criteria, including changes in best corrected visual acuity (BCVA), as well as leakage in fluorescein angiography (FA), morphologic findings in optical coherence tomography (OCT), and/or in ophthalmologic fundus examination.[15] Recently, OCT has become a valuable, if not the most valuable tool in the diagnosis and monitoring of patients with nAMD.[8,16,17] The role of morphological OCT parameters for visual function is currently being discussed very controversially.

In various pharmaceutical studies, as well as in clinical practice, a reduction in central retinal thickness (CRT) was considered a therapeutic success even though it has been shown that a decrease in retinal thickness is not necessarily related to superior retinal function. The dissociation between CRT and BCVA highlights the need for OCT parameters, which better indicate the functional success of therapy.[9,18,19] Some authors have identified structural changes relevant for visual function based on the analysis of time-domain OCT (TD-OCT) scans.[13,20–22] Since spectral-domain OCT (SD-OCT) has largely replaced TD-OCT due to better image quality and faster imaging speed, a more detailed analysis of the retinal microstructure has become available.[23–26] Despite an abundant offer of morphologic features in the clinical management of patients, however,

the diagnostic "view" of the treating ophthalmologist alone is rather inconsistent and substantial inconsistencies were noted even between retina experts.[27] Solid and quantitative automated algorithms and procedures are more promising to provide fast and reliable insights into structure-function correlations.

In this prospective study, the influence of ranibizumab therapy on the foveal microstructure has been investigated using a quantitative analysis of SD-OCT scans through the entire fovea of treated individuals over a continuous 2-year follow-up period. The foveal center was analyzed systematically in this study for two reasons: first, the foveal center is the most important retinal area for distance visual acuity and, second, an automated algorithm for an evaluation of the retinal microstructure is more likely to be technically feasible and clinically implementable in a smaller section of the central retina.[28,29] Attention has been directed to lesions of the external limiting membrane (ELM) and the ellipsoid zone (EZ) (formerly known as the boundary between the inner and the outer segments)[30] of the photoreceptors, as both of these lines have been shown to reflect photoreceptor function and may explain distinct recovery patterns of visual acuity.[31–36] Other OCT features typical of nAMD, like the presence of subretinal fluid (SRF), retinal pigment epithelium detachment (PED), drusen, intraretinal cysts, subretinal mass, and subretinal pigment epithelium mass were also evaluated in this study.

Methods

Patients and Treatment

Twenty eyes of 20 consecutive patients with treatment-naïve nAMD were included in this observational case series. Every patient gave written informed consent before study enrollment. The study protocol was approved by the local ethics committee and adhered to the ethical tenets of the Declaration of Helsinki.

All patients were examined monthly in our clinic and received standardized intravitreal injections of 0.5 mg ranibizumab[37] for 12 months (monthly dosing regimen or an as needed [pro re nata (PRN)] regimen with monthly monitoring) followed by an extended follow-up regimen and were followed for 24 months (±2 months). The flexible regimens (PRN and extended follow-up) were based on the following retreatment criteria:

A loss of BCVA of more than four Early Treatment Diabetic Retinopathy Study (ETDRS) letters, sub- or intraretinal fluid on OCT imaging, development of new or increase of preexisting PED by SD-OCT, sub- or intraretinal hemorrhage by funduscopy, or leakage in FA examination. A complete clinical examination with BCVA testing, slit-lamp biomicroscopy, ophthalmoscopy, and SD-OCT, was performed in monthly intervals during the first year and, dependent on the disease activity, monthly or 2-monthly during the second year. After the first year of follow-up, intervals between the study visits could be extended to 2 months, if the patients showed no sign of disease activity for three consecutive monthly visits.

Fluorescein angiography was performed at baseline to confirm the presumed diagnosis of nAMD and when necessary to detect disease activity (e.g., in visual loss without OCT changes).

OCT Evaluation Method

Spectral domain OCT images were obtained using the Spectralis HRA+OCT imaging device (Heidelberg Engineering, Heidelberg, Germany) at every patient visit. Volume scans were obtained consisting of 49 horizontal B scans with 20 averaged frames per B scan centered over the fovea (spacing between B scans 120 μm) and the integrated follow-up mode of the device was used to ensure that the exact same retinal area was imaged at every follow-up visit. Retinal thickness within the central circle of the ETDRS-grid (diameter of 1 mm) centered over the fovea (CRT) was measured using the incorporated software of the Spectralis-OCT.

A proprietary software (OCT-toolkit version 1.6, provided by the Vienna Reading Center) was used for microstructural analysis, allowing the investigator to manually delineate areas of interest in every cross-sectional image of a defined three-dimensional dataset. The software has recently been described by Sayegh et al.[38] Two-dimensional areas (in mm^2) of the specific regions of interest were calculated automatically by interpolating between the manually delineated areas in the single B-scans. To exclude an individual reader bias, readings were done by two different retina experts (PR, JM), who graded the OCT B-scans independently at different time points in different orders.

The present study evaluated the microstructure of the central foveal 1 mm^2 (consisting of eight consecutive horizontal B scans) for specific morphologic findings (listed below) at baseline, at month 12 (±1 month), and at month 24 (±2 months) using the following method: 500 μm on either side of the center of the fovea was measured in each of the eight central horizontal B scans, resulting in an area of 960 × 1000 μm (height × width) centered over the fovea. The height of the volume stack resulted from the B-scan spacing of 120 μm. These dimensions were chosen to achieve the goal of precisely investigating the central square millimeter of the macula (Figs. 1–3).

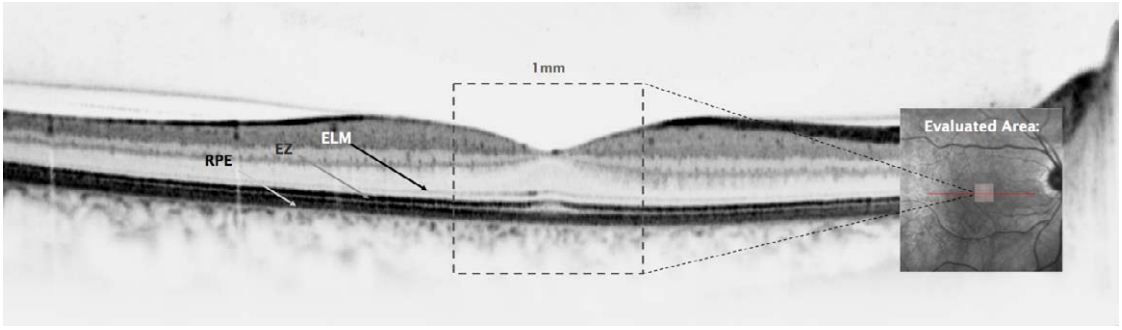

Figure 1. Horizontal OCT B-scan of a healthy retina and the corresponding en face SLO-image illustrating the size of the evaluated area highlighted in *red*. The *red horizontal line* in the en face SLO-image shows the B-scan position. In this subject, the ELM and the EZ are visualized as continuous lines throughout the whole scan.

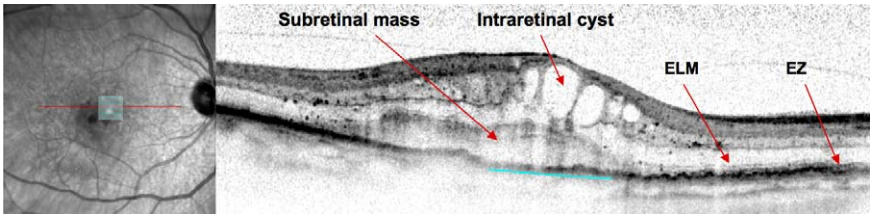

FIGURE 2. Horizontal B-scan and the corresponding en face SLO image before the first ranibizumab injection illustrating some of the evaluated OCT features. In this cross-sectional image, an ELM-disruption is highlighted in *blue* in the OCT B-scan and in the en face image. The *red horizontal line* in the en face SLO-image illustrates the B-scan position. Intraretinal cysts and a subretinal mass can be observed. Both the ELM as well as the EZ are absent within the central 1000 μm.

Definition and Identification of Morphologic Parameters

Within the foveal area, the following pathologies were recorded and quantified systematically:

1. Condition of the ELM: ELM present, discontinuous, not present
2. Condition of the EZ: EZ present, discontinuous, not present
3. Presence of SRF
4. Presence of PED
5. Presence of foveal drusen
6. Presence of intraretinal cysts
7. Presence of subretinal mass (hyperreflective material located between the neuroretina and the RPE)
8. Presence of subretinal pigment epithelium mass (sub-RPE mass; hyperreflective material located below the RPE)

The EZ was defined as the second hyperreflective band above the RPE (Figs. 1–3) (the first hyperreflective band above the RPE is believed to represent interdigitations between the photoreceptor outer segments and the RPE cells[39]). The ELM was defined as a discrete hyperreflective band at the outermost border of the outer nuclear layer, located above the EZ (Figs. 1–3). Subretinal fluid was diagnosed in areas where a non-reflective space was present between the posterior boundary of the neuroretina and the RPE (Fig. 3).

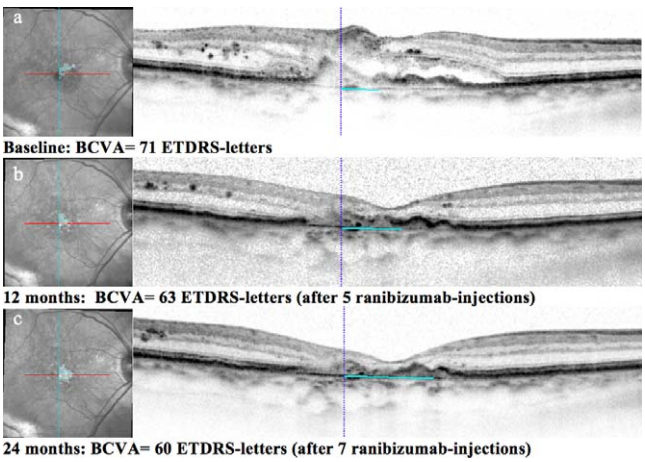

FIGURE 3. Horizontal OCT B scans and the corresponding en face SLO-images taken from the same patient at baseline (**A**), 12 months (**B**), and 2 years (**C**). The *red horizontal lines* in the en face images illustrate the B-scan positions. The *blue vertical lines* on the B scans and on the SLO en face images show the left border of the evaluated area. Manually delineated areas of ELM alteration are highlighted in *blue* in the B scans and in the en face SLO images.

Intraretinal cysts were identified as round, nonreflective to minimally reflective spaces within the neuroretina (Fig. 2). Pigment epithelium detachment was defined as a focal elevation of the RPE with a minimum width of 400 μm measured at the base or a minimum height of 200 μm measured from the choriocapillaris to the RPE.

In this study, the total areas (quantified in mm^2) of the pathologies described above were correlated with best-corrected visual acuity (BCVA) results from the corresponding visits and the change to baseline, respectively. In contrast to most studies, analyzing photoreceptor status in SD-OCT only qualitatively, we managed to directly assess the relationship between quantitatively evaluated microstructural findings and functional changes (ETDRS letter score).[31–36,40–43]

For statistical analyses, IBM SPSS statistics version 20 (IBM SPSS Statistics, IBM Corporation, Chicago, IL, USA) was used. To assess interobserver variability for all measured OCT findings, intraclass correlation coefficients (ICCs) were calculated. Univariate and stepwise multivariate regression analyses were used to calculate the relevant influence of each of the independent variables on visual acuity. A P value less than 0.05 was considered statistically significant.

RESULTS

A total of 480 foveal B scans of 20 eyes of 20 consecutive patients (14 female, 6 male) with treatment-naïve nAMD receiving standardized monthly intravitreal therapy (13 eyes) or initial PRN treatment (7 eyes) for 12 months using ranibizumab followed by 12 months of an extended follow-up ranibizumab regimen were analyzed. The mean age was 79.3 ± 7.8 years (range 62–89). The mean baseline BCVA was 58.9 (±16.2) ETDRS letters. After 12 months (±1 month) and 24 months (±2 months), mean BCVA was 66.0 (±16.5) ETDRS letters and 59.9 (±16.5) ETDRS letters, respectively.

Nine of the patients were diagnosed with an occult CNV lesion, six with a classic, three with a minimally classic, one with a predominantly classic, and one with a retinal angiomatous proliferation (RAP) lesion. Mean area of leakage (measured in the late phase of FA) at baseline was 4.6 ± 4.8 mm^2 (range: 0.41–18.05 mm^2).

Patterns of Visual Gain, Maintenance, and Loss

Three groups of patients (losers, gainers, and maintainers) were distinguished depending on their visual acuity change from baseline to month 24. "Maintainers" were defined as patients who responded to treatment with ranibizumab and experienced a visual acuity improvement initially but whose BCVA declined during the 2-year follow-up, resulting in a visual acuity of ±5 ETDRS letters at 24 months compared with baseline. Patients who gained more than five ETDRS letters after 24

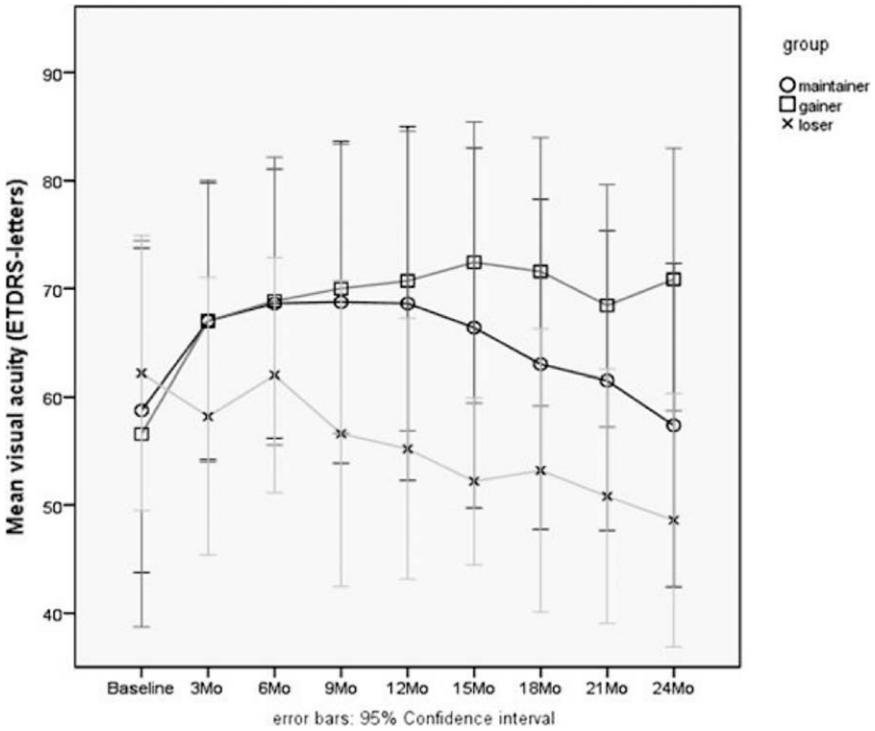

FIGURE 4. Mean visual acuity change over time from baseline to month 24 by functional subgroup (losers, gainers, and maintainers).

months were defined as "gainers," and patients who lost more than five ETDRS letters were defined as "losers" (Fig. 4).

In our study population, five visual acuity losers (mean ETDRS letter change after 24 months: –13.6 [±7.4]), eight maintainers (mean ETDRS letter change: –1.4 [±5]), and seven gainers (mean ETDRS letter change: +14.3 [±11.9]) were documented. Mean CRT values for each subgroup are illustrated in Figure 5. For characteristics other than evaluated OCT findings, see the Table. However, no significant influence of any of those parameters on visual function was identified.

The strongest increase of CRT following an initial decrease was observed in the "maintainer" group, a less-pronounced increase was observed in the "gainer" group, and further decrease after 12 months was observed in the "loser" group (Figs. 4, 5).

Univariate regression analysis was performed for CRT and visual acuity at baseline, 12 months, and 24 months. Visual acuity showed a significant dependence on CRT only at baseline ($R = –0.612$; $P = 0.004$).

Correlation of Function and Area of Morphologic Alteration by OCT

Analysis of 480 horizontal B scans for eight different OCT features typical of nAMD demonstrated the following results (Fig. 6).

In general, an excellent intergrader agreement could be achieved. The intergrader agreement was best for SRF (ICCs were 0.988 at baseline, 0.993 at 1 and 0.994 at 2 years) and intraretinal cysts (ICCs were 0.989 at baseline, 0.952 at 1 and 0.997 at 2 years) and less effective for the evaluation of the EZ (ICCs were 0.657 at baseline, 0.780 at 1 and 0.878 at 2 years).

At baseline (i.e., in the native AMD condition), the areas of ELM alteration ($R = –0.67$; $P = 0.001$), EZ alteration ($R = –0.656$; $P = 0.002$), intraretinal cysts ($R = –0.446$; $P = 0.049$), subretinal mass ($R = –0.641$; $P = 0.002$), and CRT ($R = –0.612$; $P = 0.004$) were significant parameters influencing BCVA in the univariate regression analyses.

In general, under treatment, features related to the exudative activity of nAMD disease, such as intraretinal cysts, SRF, or PED, resolved initially under the tighter regimen with monthly dosing/monitoring followed by recurrence in the looser extended follow-up regimen with less dosing/monitoring of the second year. Structural changes, such as alterations of the ELM and EZ lines, remained stable, the area of a subretinal solid mass (i.e., scarring tissue) increased over time.

At 12 months, the area of ELM alteration ($R = –0.846$; $P < 0.001$), EZ alteration ($R = –0.695$; $P = 0.001$) and subretinal mass ($R = –0.627$; $P = 0.003$) were significantly affecting BCVA.

At 24 months, the area of ELM alteration ($R = –0.778$; $P < 0.001$), EZ alteration ($R = –0.673$; $P = 0.001$), and subretinal mass ($R = –0.577$; $P = 0.002$) and SRF recurring during the extended follow-up regimen ($R = 0.618$; $P = 0.004$) had a significant impact on BCVA in the univariate analyses.

In the stepwise multivariate regression analysis, the area of ELM alteration, the area of intraretinal cysts and CRT were significant variables influencing visual acuity at baseline ($R = –0.827$; $R^2 = 0.684$; $P < 0.001$).

At 12 months and at 24 months, the area of ELM alteration was the only significant factor to directly influence visual function with $R = –0.846$ and $R^2 = 0.716$ at a significance level of $P < 0.001$ at 12 months and $R = –0.778$ and $R^2 = 0.606$ at a significance level of $P < 0.001$ at 24 months.

None of the OCT parameters measured in this study were significantly correlating with the prospective change in visual acuity from baseline to 12 months, from baseline to 24 months, or from 12 months to 24 months, respectively. Hence, none of the OCT parameters could be identified as a predictor for an increase or decrease in BCVA for the individual patient.

In the univariate linear regression analysis, visual acuity at month 12 and month 24 were significantly correlating with baseline ELM alteration area ($R = –0.696$; $P = 0.001$ and $R = –0.558$; $P = 0.01$), EZ alteration area ($R = –0.721$; $P < 0.001$ and $R = –0.646$; $P = 0.02$), SRF area ($R = 0.505$; $P = 0.023$ and R

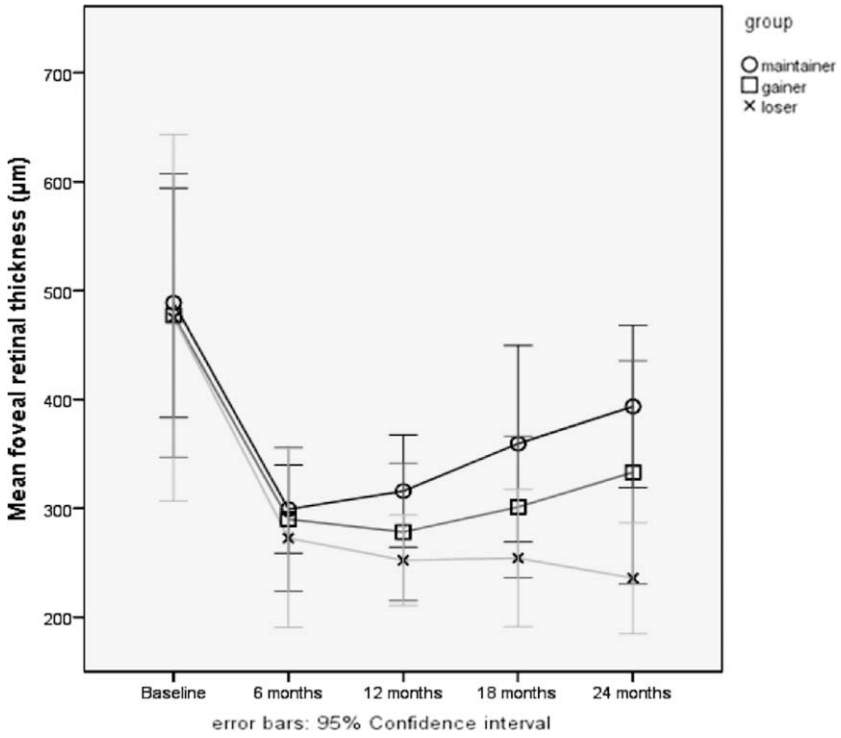

Figure 5. Time course of mean foveal retinal thickness change by functional subgroup (losers, gainers, and maintainers).

$= 0.556$; $P = 0.011$) and subretinal mass extension ($R = -0.58$; $P = 0.007$ and $R = -0.756$; $P < 0.001$).

In the multivariate linear regression analysis, EZ alteration area at baseline was the only parameter significantly correlating with visual acuity at month 12 ($R = -0.721$; $P < 0.001$) and subretinal mass extension at baseline was the only parameter significantly correlating with visual acuity at month 24 ($R = -0.756$; $P < 0.001$).

Table. Characteristics by Functional Subgroup Other Than Quantitatively Evaluated OCT-Findings, Including Presence of Hemorrhage, RPE Atrophy, or Fibrosis in the Macula, Angiographic CNV Type, and Size (mm^2) at Baseline as Measured in Late-Phase FA, Retinal Thickness at Baseline, and Visual Acuity

	Maintainer, $n = 8$			Gainer, $n = 7$			Loser, $n = 5$		
	Count	Mean	SD	Count	Mean	SD	Count	Mean	SD
Macular hemorrhage present									
Baseline	3			3			3		
24 mo	0			0			0		
Macular RPE atrophy present									
Baseline	1			1			1		
24 mo	1			3			2		
Macular fibrosis present									
Baseline	2			1			0		
24 mo	4			3			4		
CNV-type:									
Occult	5			2			2		
Classic	2			3			1		
RAP	0			1			0		
Predominantly classic	0			0			1		
Minimally classic	1			1			1		
Size of CNV complex in FA at baseline, mm^2		5.39	5.47		3.15	3.18		5.47	6.1
Retinal thickness baseline, µm		488.75	125.91		477.00	140.86		475.00	135.51
BCVA baseline, ETDRS-letters		58.75	17.93		56.57	19.29		62.2	10.23
BCVA 12 months, ETDRS-letters		68.63	19.57		70.71	14.96		55.2	9.71
BCVA 24 months, ETDRS-letters		57.38	17.88		70.86	13.12		48.6	9.45

Investigative Ophthalmology & Visual Science

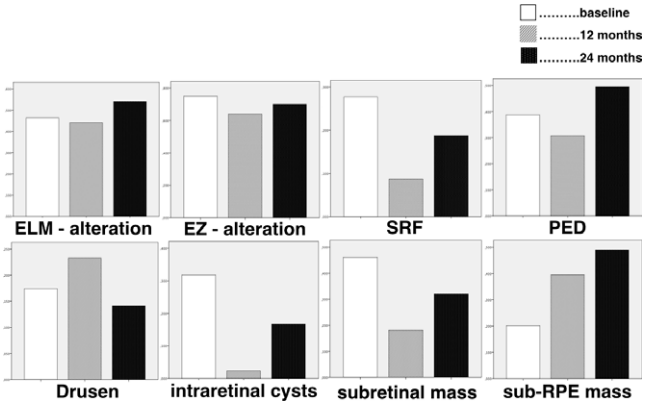

FIGURE 6. Mean area of the evaluated OCT features within the evaluated foveal area at baseline, and after 12 and 24 months (mm^2).

DISCUSSION

The present study analyzed the pathomorphologic characteristics of native neovascular AMD at baseline and under ranibizumab therapy with a focus on microstructural foveal alteration and its correlation to visual function.

In general, in the cases analyzed in this study, a decrease in CRT was generally not associated with improved visual function (Figs. 3–5), highlighting the necessity of additional morphologic parameters allowing identification of the functional condition of nAMD patients undergoing antiangiogenic therapy.

Using OCT analysis based on identification of defined qualitative features, as well as their quantitative extension, the area of ELM alteration was shown to have a significant impact on visual acuity at baseline, at 12 months, and at 24 months. Moreover, in the stepwise linear regression analyses, the ELM condition was the most important factor to influence visual function at baseline (i.e., the native nAMD condition and during follow-up), which is consistent with the results of previous studies using different nonquantitative approaches.[31,32,34,36,42,44] In eyes with nAMD, retinal detachment, macular hole, or retinal vein occlusion, the ELM, which is believed to represent the junctional zone between Müller cells and photoreceptors, seems to be a hallmark for photoreceptor function and its condition may directly reflect the potential for visual function and/or recovery.[33,34,45–48]

Different studies have been conducted to elucidate the role of the ELM for visual function and for the preservation of the retinal structure, one of which suggested that the ELM acts as a barrier for macromolecules.[49,50] Murakami et al.[51] hypothesized that a disruption of the ELM could lead to osmotic imbalance and consecutively to photoreceptor dysfunction. This hypothesis has been confirmed in a recent study by Uji et al.,[52] by demonstrating that hyperreflective foci in the outer retinal layers are significantly correlating with ELM disruption in eyes with diabetic macular edema. Müller cells play a crucial role for retinal function while regulating neuronal metabolism and interacting with photoreceptor cells.[53] In a recent article, Franze et al.[54] postulated that Müller cells act similar to natural optical fibers guiding light toward the photoreceptors, thus compensating for the "inverse" layering of the retina, with the photoreceptors being the retinal layer farthest away from light entering the eye. Photoreceptor cells are covered by several layers of different cell types with different refractive indices, which would create a distorted picture if Müller cells would not compensate for this problem. Therefore, structural damage to the adherent junctions between Müller cells and photoreceptors (i.e., the ELM) would compromise both the structural barrier as well as their functional interaction.

Wakabayashi et al.[46,55] pointed out that the condition of the ELM would reflect the integrity of photoreceptor cell bodies, whereas the status of the EZ line may rather reflect the integrity of the photoreceptor outer segments, explaining why the ELM layer represents a better predictor for photoreceptor restoration. In diseases with severe photoreceptor damage (as in AMD), the EZ line seems to be too indistinct to be particularly useful as a reliable predictor for BCVA.[34,46,55]

In our study, a significant correlation was observed between the EZ alteration area and BCVA in the univariate linear regression analysis at baseline, at 12 months, and at 24 months; however, the condition of the EZ structure did not offer consistent significant correlations to BCVA in the multivariate linear regression analysis. On the other hand, subretinal fluid also showed a significant positive correlation with BCVA at month 24. This may, however, be due to the high rate of recurrent SRF in the extended follow-up regimen applied in the second year and demonstrates a potential impact of the performed therapeutic regimen. Although this finding might appear counterintuitive at first glance, one possible hypothesis might be that photoreceptors surrounded by fluid suffer less structural damage than those embedded in scarred tissue.

However, none of the OCT parameters investigated in this study was a significant predictor for the change from baseline to mid- (12 months) or long-term BCVA (24 months). The overall results suggest that patients with more extensive areas of ELM alteration, EZ alteration, or subretinal mass may result in a worse prognosis regarding mid- and long-term visual outcome; however, a solid prognosis, whether the patient will eventually be a loser, gainer, or maintainer cannot be made in a conclusive way based on this analysis.

The software developed for microstructural analysis proved to provide useful orientational parameters for further analysis on a larger base. The authors of this study are aware of the limited number of patients that were included in this study. Whether the foveal findings of this study hold true for the entire macula in a larger population still has to be confirmed in larger studies. As it was necessary for the detailed analysis of OCT parameters to have excellent image quality, only a limited number of patients could be enrolled in this study. Moreover, as the evaluation of only the foveal microstructure in correlation with BCVA was the aim of this study, patients with obvious excentric fixation had to be excluded, which limited the number of eligible patients even further. The meticulous and time-consuming method of analysis also limited the number of patients included in this study.

In conclusion, this study showed the importance of ELM integrity for visual acuity in patients with neovascular AMD treated with anti-VEGF agents. A systematic, quantitative assessment of the central retinal microstructure may offer the optimal strategy to guide the treatment management in neovascular AMD. However, until reliable automated programs for detailed OCT-analysis for pathologic structures exist, researchers and clinicians have to make their decisions based on personal, subjective evaluation of image data. With the reproducible identification of morphologic factors relevant for visual performance, reliable automated algorithms may be designed to guide therapeutic strategies with optimal outcomes, pragmatic procedures to facilitate patients' and physicians lives for one of the leading diseases of modern civilizations.

Acknowledgments

Disclosure: **P. Roberts**, None; **T.J. Mittermueller**, None; **A. Montuoro**, None; **F. Sulzbacher**, None; **M. Munk**, None; **S. Sacu**, None; **U. Schmidt-Erfurth**, None

References

1. Bloch SB, Larsen M, Munch IC. Incidence of legal blindness from age-related macular degeneration in Denmark: year 2000 to 2010. *Am J Ophthalmol*. 2012;153:209–213. e2.
2. Bressler NM, Doan QV, Varma R, et al. Estimated cases of legal blindness and visual impairment avoided using ranibizumab for choroidal neovascularization: non-Hispanic white population in the United States with age-related macular degeneration. *Arch Ophthalmol*. 2011;129:709–717.
3. Buch H, Vinding T, La Cour M, Appleyard M, Jensen GB, Nielsen NV. Prevalence and causes of visual impairment and blindness among 9980 Scandinavian adults: the Copenhagen City Eye Study. *Ophthalmology*. 2004;111:53–61.
4. Congdon N, O'Colmain B, Klein R, et al. Causes and prevalence of visual impairment among adults in the United States. *Arch Ophthalmol*. 2004;122:477–485.
5. Klein R, Peto T, Bird A, et al. *The epidemiology of age-related macular degeneration*. *Am J Ophthalmol*. 2004;137:486–495.
6. Bird AC, Bressler NM, Bressler SB, et al. An international classification and grading system for age-related maculopathy and age-related macular degeneration. The International ARM Epidemiological Study Group. *Surv Ophthalmol*. 1995;39:367–374.
7. Eyetech Study Group. Anti-vascular endothelial growth factor therapy for subfoveal choroidal neovascularization secondary to age-related macular degeneration: phase II study results. *Ophthalmology*. 2003;110:979–986.
8. Keane PA, Tufail A, Patel PJ. Management of neovascular age-related macular degeneration in clinical practice: initiation, maintenance, and discontinuation of therapy. *J Ophthalmol*. 2011;2011:752543.
9. Mitchell P, Korobelnik JF, Lanzetta P, et al. Ranibizumab (Lucentis) in neovascular age-related macular degeneration: evidence from clinical trials. *Br J Ophthalmol*. 2010;94:2–13.
10. Rosenfeld PJ, Brown DM, Heier JS, et al. Ranibizumab for neovascular age-related macular degeneration. *N Engl J Med*. 2006;355:1419–1431.
11. Schmidt-Erfurth U, Eldem B, Guymer R, et al. Efficacy and safety of monthly versus quarterly ranibizumab treatment in neovascular age-related macular degeneration: the EXCITE study. *Ophthalmology*. 2011;118:831–839.
12. Schmidt-Erfurth UM, Richard G, Augustin A, et al. Guidance for the treatment of neovascular age-related macular degeneration. *Acta Ophthalmol Scand*. 2007;85:486–494.
13. Grunwald JE, Daniel E, Huang J, et al. Risk of geographic atrophy in the comparison of age-related macular degeneration treatments trials. *Ophthalmology*. 2014;121:150–161.
14. Young M, Chui L, Fallah N, et al. Exacerbation of choroidal and retinal pigment epithelial atrophy afteranti-vascular endothelial growth factor treatment in neovascular age-related macular degeneration. *Retina*. 2014;34:1308–1315.
15. Katz G, Giavedoni L, Muni R, et al. Effectiveness at 1 year of monthly versus variable-dosing intravitreal ranibizumab in the treatment of choroidal neovascularization secondary to age-related macular degeneration. *Retina*. 2012;32:293–298.
16. Harding SP. Neovascular age-related macular degeneration: decision making and optimal management. *Eye (Lond)*. 2010;24(3);497–505.
17. Kulkarni AD, Kuppermann BD. Wet age-related macular degeneration. *Adv Drug Deliv Rev*. 2005;57:1994–2009.
18. Ciulla TA, Rosenfeld PJ. Antivascular endothelial growth factor therapy for neovascular age-related macular degeneration. *Curr Opin Ophthalmol*. 2009;20:158–165.
19. Lalwani GA, Rosenfeld PJ, Fung AE, et al. A variable-dosing regimen with intravitreal ranibizumab for neovascular age-related macular degeneration: year 2 of the PrONTO Study. *Am J Ophthalmol*. 2009;148:43–58.e1.
20. Daniel E, Toth CA, Grunwald JE, et al. Risk of scar in the comparison of age-related macular degeneration treatments trials. *Ophthalmology*. 2014;121:656–666.
21. Jaffe GJ, Martin DF, Toth CA, et al. Macular morphology and visual acuity in the comparison of age-related macular degeneration treatments trials. *Ophthalmology*. 2013;120:1860–1870.
22. Ying GS, Huang J, Maguire MG, et al. Baseline predictors for one-year visual outcomes with ranibizumab or bevacizumab for neovascular age-related macular degeneration. *Ophthalmology*. 2013;120:122–129.
23. Choma M, Sarunic M, Yang C, Izatt J. Sensitivity advantage of swept source and Fourier domain optical coherence tomography. *Opt Express*. 2003;11:2183–2189.
24. de Boer JF, Cense B, Park BH, Pierce MC, Tearney GJ, Bouma BE. Improved signal-to-noise ratio in spectral-domain compared with time-domain optical coherence tomography. *Opt Lett*. 2003;28:2067–2069.
25. Leitgeb R, Hitzenberger C, Fercher A. Performance of Fourier domain vs. time domain optical coherence tomography. *Opt Express*. 2003;11:889–894.
26. Luviano DM, Benz MS, Kim RY, et al. Selected clinical comparisons of spectral domain and time domain optical coherence tomography. *Ophthalmic Surg Lasers Imaging*. 2009;40:325–328.
27. Framme C, Panagakis G, Walter A, et al. Interobserver variability for retreatment indications after Ranibizumab loading doses in neovascular age-related macular degeneration. *Acta Ophthalmol*. 2012;90:49–55.
28. Pilch M, Stieger K, Wenner Y, et al. Automated segmentation of pathological cavities in optical coherence tomography scans. *Invest Ophthalmol Vis Sci*. 2013;54:4385–4393.
29. Weiter JJ, Wing GL, Trempe CL, Mainster MA. Visual acuity related to retinal distance from the fovea in macular disease. *Ann Ophthalmol*. 1984;16:174–176.
30. Spaide RF. Questioning optical coherence tomography. *Ophthalmology*. 2012;119:2203–2204.
31. Akagi-Kurashige Y, Tsujikawa A, Oishi A, et al. Relationship between retinal morphological findings and visual function in age-related macular degeneration. *Graefes Arch Clin Exp Ophthalmol*. 2012;250:1129–1136.
32. Hayashi H, Yamashiro K, Tsujikawa A, Ota M, Otani A, Yoshimura N. Association between foveal photoreceptor integrity and visual outcome in neovascular age-related macular degeneration. *Am J Ophthalmol*. 2009;148:83–89.e1.
33. Landa G, Gentile RC, Garcia PM, Muldoon TO, Rosen RB. External limiting membrane and visual outcome in macular hole repair: spectral domain OCT analysis. *Eye (Lond)*. 2012;26:61–69.
34. Oishi A, Hata M, Shimozono M, Mandai M, Nishida A, Kurimoto Y. The significance of external limiting membrane status for visual acuity in age-related macular degeneration. *Am J Ophthalmol*. 2010;150:27–32.e1.
35. Ooka E, Mitamura Y, Baba T, Kitahashi M, Oshitari T, Yamamoto S. Foveal microstructure on spectral-domain optical coherence tomographic images and visual function after macular hole surgery. *Am J Ophthalmol*. 2011;152:283–290.e1.
36. Landa, G, Su E, Garcia PM, Seiple WH, Rosen RB. Inner segment-outer segment junctional layer integrity and corresponding retinal sensitivity in dry and wet forms of age-related macular degeneration. *Retina*. 2011;31:364–370.
37. Ta CN. Minimizing the risk of endophthalmitis following intravitreous injections. *Retina*. 2004;24:699–705.

38. Sayegh RG, Simader C, Scheschy U, et al. A systematic comparison of spectral-domain optical coherence tomography and fundus autofluorescence in patients with geographic atrophy. *Ophthalmology*. 2011;118:1844–1851.
39. Zawadzki RJ, Jones SM, Olivier SS, et al. Adaptive-optics optical coherence tomography for high-resolution and high-speed 3D retinal in vivo imaging. *Opt Express*. 2005;13:8532–8546.
40. Domalpally A, Peng Q, Danis R, Blodi B, Scott IU, Ip M. Association of outer retinal layer morphology with visual acuity in patients with retinal vein occlusion: SCORE Study Report 13. *Eye (Lond)*. 2012;26:919–924.
41. Kim, HJ, Kang JW, Chung H, Kim HC. Correlation of foveal photoreceptor integrity with visual outcome in idiopathic epiretinal membrane. *Curr Eye Res*. 2014;39:626–633.
42. Oishi A, Shimozono M, Mandai M, Hata M, Nishida A, Kurimoto Y. Recovery of photoreceptor outer segments after anti-VEGF therapy for age-related macular degeneration. *Graefes Arch Clin Exp Ophthalmol*. 2013;251:435–440.
43. Okamoto F, Sugiura Y, Okamoto Y, Hiraoka T, Oshika T. Metamorphopsia and optical coherence tomography findings after rhegmatogenous retinal detachment surgery. *Am J Ophthalmol*. 2014;157:214–220.e1.
44. Pappuru RR, Ouyang Y, Nittala MG, et al. Relationship between outer retinal thickness substructures and visual acuity in eyes with dry age-related macular degeneration. *Invest Ophthalmol Vis Sci*. 2011;52:6743–6748.
45. Shin HJ, Chung H, Kim HC. Association between foveal microstructure and visual outcome in age-related macular degeneration. *Retina*. 2011;31:1627–1636.
46. Wakabayashi T, Oshima Y, Fujimoto H, et al. Foveal microstructure and visual acuity after retinal detachment repair: imaging analysis by Fourier-domain optical coherence tomography. *Ophthalmology*. 2009;116:519–528.
47. Wolf-Schnurrbusch UE, Ghanem R, Rothenbuehler SP, Enzmann V, Framme C, Wolf S. Predictors of short-term visual outcome after anti-VEGF therapy of macular edema due to central retinal vein occlusion. *Invest Ophthalmol Vis Sci*. 2011;52:3334–3337.
48. Yamaike N, Tsujikawa A, Ota M, et al. Three-dimensional imaging of cystoid macular edema in retinal vein occlusion. *Ophthalmology*. 2008;115:355–362.e2.
49. Bunt-Milam AH, Saari JC, Klock IB, Garwin GG. Zonulae adherentes pore size in the external limiting membrane of the rabbit retina. *Invest Ophthalmol Vis Sci*. 1985;26:1377–1380.
50. Marmor MF. Mechanisms of fluid accumulation in retinal edema. *Doc Ophthalmol*. 1999;97:239–249.
51. Murakami T, Nishijima K, Sakamoto A, Ota M, Horii T, Yoshimura N. Association of pathomorphology, photoreceptor status, and retinal thickness with visual acuity in diabetic retinopathy. *Am J Ophthalmol*. 2011;151:310–317.
52. Uji A, Murakami T, Nishijima K, et al. Association between hyperreflective foci in the outer retina, status of photoreceptor layer, and visual acuity in diabetic macular edema. *Am J Ophthalmol*. 2012;153:710–717.
53. Bringmann A, Pannicke T, Grosche J, et al. Muller cells in the healthy and diseased retina. *Prog Retin Eye Res*. 2006;25:397–424.
54. Franze K, Grosche J, Skatchkov SN, et al. Muller cells are living optical fibers in the vertebrate retina. *Proc Natl Acad Sci U S A*. 2007;104:8287–8292.
55. Wakabayashi T, Fujiwara M, Sakaguchi H, Kusaka S, Oshima Y. Foveal microstructure and visual acuity in surgically closed macular holes: spectral-domain optical coherence tomographic analysis. *Ophthalmology*. 2010;117:1815–1824.

Appendix

The Macula Study Group Vienna

Department of Ophthalmology, Medical University of Vienna, Vienna, Austria

Stefan Sacu, MD
Wolf Buehl, MD
Roman Dunavoelgyi, MD
Katharina Eibenberger, MD
Sandra Rezar, MD
Markus Ritter, MD
Philipp Roberts, MD
Guenther Weigert, MD
Michael Georgopoulos, MD
Ursula M. Schmidt-Erfurth, MD

Investigative Ophthalmology & Visual Science